ROTOR FAULT COMPENSATION AND DETECTION IN A SENSORLESS INDUCTION MOTOR DRIVE*

SZYMON BEDNARZ

Wrocław University of Science and Technology, Department of Electrical Machines,
Drives and Measurements, Wybrzeże Wyspiańskiego 27, 50-370 Wrocław, Poland,
e-mail address: szymon.bednarz@pwr.edu.pl

Abstract: The compensation and detection analysis of rotor faults in a sensorless induction motor drive system with an additional rotor resistance estimator has been conducted and the influence of the rotor faults on the properties of such system has been examined. The rotor flux vector and rotor speed have been reconstructed by the MRAS^{CC} estimator. The drive was tested for various conditions. Simulation tests were performed in the direct field oriented control (DFOC) structure realized in the MATLAB/Simulink software.

Keywords: rotor faults, DFOC, speed estimator, MRAS, parameter estimator

1. INTRODUCTION

Modern induction motor (IM) drive systems are widely used in various industrial applications. Advanced control structures like direct field oriented control (DFOC) or direct torque control with space vector modulation (DTC-SVM) require the state variable estimation [1, 8]. During last few years, limitation of mechanical and electrical variables sensors can be observed [1]. A proper choice of speed and flux estimator is very complicated and depends on the requirements of the drive system. In terms of safety, it is very important for state variable estimators to be robust for the variations of motor parameters.

This problem is especially important in the fault tolerant control systems (FTCS) [2, 3, 5, 7]. The general idea of this problem was described in detail elsewhere [5]. One of the FTCS are active systems which use detectors or observers to identify the failure condition [2–5]. The main goal is stable operation of the drive system which can be obtained by using additional estimators [4, 5, 7]. In the induction motor drive system based on an active detection system which can be resistant to the speed sensor faults, the rotor speed estimator must be used [5]. When the rotor of induction motor is

_____

broken, the rotor resistance is different than the nominal value [1, 6, 12]. In each sensorless IM drive, the symptoms of this fault can be observed [1, 10]. Because all of the speed estimation techniques are more or less sensitive to the motor parameter changes, the rotor speed can be calculated with some steady state error [1, 9, 10] during this faulted conditions. In the FTC drives, the diagnostic process depends on the difference between the measured and estimated speed, the faults of the rotor bars can provoke false detection of the speed sensor fault [5]. From this reason, the speed estimator in the FTC system should be extended to the rotor resistance estimator [1]. The estimated rotor resistance can be also used as an additional parameter for the drive system diagnostics [1, 6, 12].

The main goal of the paper is the analysis of the possibility of detection and compensation of the rotor faults in the sensorless induction motor drive system controlled by the direct field oriented controlled method. For the rotor flux and speed estimation the $MRAS^{CC}$ estimator with an additional rotor resistance estimator was used. Simulation tests were performed in the MATLAB/Simulink software. The Euler method was used as the numerical integration method with the step size $t = 0.00001$ s.

2. CONTROL STRUCTURE AND SPEED ESTIMATOR

The general scheme of the sensorless the DFOC structure of the induction motor drive is presented in Fig. 1 [8]. The structure contains two separate control loops, the former contains a rotor flux controller and the latter contains a rotor speed controller. In this structure, the PI controllers were used. In the case of supplying the IM from a voltage inverter, it is necessary to use decoupling block e_x, e_y. The decoupling signals e_x, e_y were calculated using equations described in detail in [8]. For the proper operation of the system, the state variable estimators should be used.

Fig. 1. Sensorless DFOC control structure for induction motor [8]

The rotor flux and speed are reconstructed by a MRAS[CC] estimator based on the model reference adaptive system [1, 9]. Figure 2 shows a block diagram of this estimator. The stator currents $i_{s\alpha}$, $i_{s\beta}$ are measured and originating from the $ABC/\alpha\beta$ transformation.
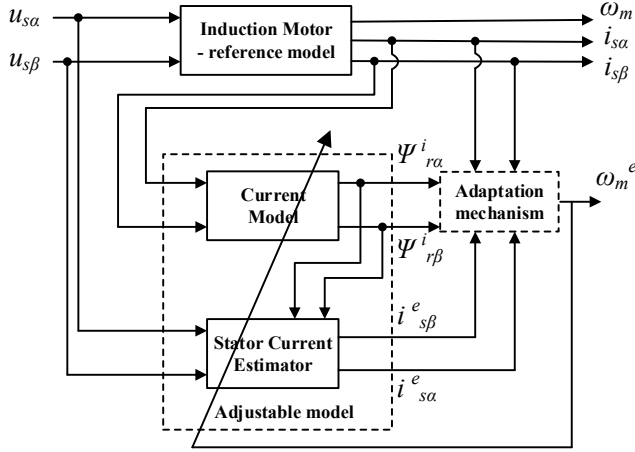

Fig. 2. Scheme of the MRAS[CC] rotor speed estimator [1]

The current model of the IM can be obtained by the equation:

$$\frac{d}{dt}\mathbf{\Psi}_r^i = \left[\frac{r_r}{x_r}(x_m\mathbf{i}_s - \mathbf{\Psi}_r^i) + j\omega_m^e\mathbf{\Psi}_r^i\right]\frac{1}{T_N} \tag{1}$$

The stator currents $\mathbf{i}_{s\alpha}^e$, $\mathbf{i}_{s\beta}^e$ are estimated as follows:

$$\frac{d}{dt}\mathbf{i}_s^e = -\frac{r_r x_m^2 + x_r^2 r_s}{\sigma T_N x_s x_r^2}\mathbf{i}_s^e + \frac{1}{\sigma T_N x_s}\mathbf{u}_s + \frac{x_m r_r}{\sigma T_N x_s x_r^2}\mathbf{\Psi}_r^i - j\omega_m^e\frac{x_m}{\sigma T_N x_s x_r}\mathbf{\Psi}_r^i \tag{2}$$

where: ω_m^e – estimated rotor angular speed, r_s, r_r, x_s, x_r, x_m – stator and rotor resistances, stator and rotor leakage reactances, and mutual reactance, respectively, $\mathbf{u}_s$, $\mathbf{i}_m^e$, $\mathbf{\psi}_r^i$, $\mathbf{u}_s$, $\mathbf{i}_s^e$, $\mathbf{\psi}_r^i$ – stator voltage, estimated stator current and rotor flux vectors, respectively, $\sigma = 1 - x_m^2/x_s x_r$, $T_N = 1/2\pi f_{sN}$.

Both models are adjusted by the estimated rotor speed which can be calculated in the adaptation mechanism:

$$\omega_m^e = K_P\left(e_{i_{s\alpha}}\Psi_{r\beta}^i - e_{i_{s\beta}}\Psi_{r\alpha}^i\right) + K_I\int\left(e_{i_{s\alpha}}\Psi_{r\beta}^i - e_{i_{s\beta}}\Psi_{r\alpha}^i\right)dt \tag{3}$$

where: $e_{i_{s\alpha,\beta}} = i_{s\alpha,\beta} - i^e_{s\alpha,\beta}$ – difference between the estimated and measured stator current, K_P, K_I – constant positive coefficients.

In the MRAS^{CC} estimator, the induction motor is used as a reference model. The measured stator current is compared with the estimated current calculated from the stator current model.

3. ROTOR RESISTANCE ESTIMATOR

In the FTC structures, the parameters of the IM should be estimated. In this paper, the system with an additional rotor resistance is described. This parameter can be different than the nominal value under different operation and during the rotor faults. The rotor resistance of the IM can be reconstructed by the estimator proposed in [13]. This concept is based on the model reference adaptive system. Figure 3 shows a block diagram of this estimator. the estimator is based on two induction motor simulators (voltage model and current model of the rotor flux). The voltage model, which is independent of the rotor resistance, is used as a reference model. The current model is used as an adjustable model, tuned by the estimated rotor resistance. In this estimator, the rotor speed is a well-known parameter, which can be measured or estimated by MRAS^{CC}.
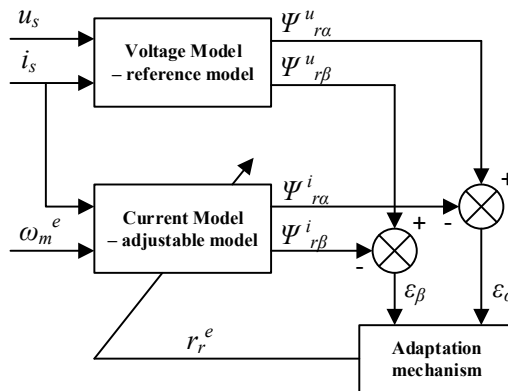
Fig. 3. Scheme of the rotor resistance estimator [13]

The quality of estimation depends on the minimization of the estimation error of the rotor flux components by the current model.

The errors ε_α and ε_β can be obtained from equations:

$$\begin{cases} \varepsilon_\alpha = \psi^u_{r\alpha} - \psi^i_{r\alpha}, \qquad \varepsilon_\beta = \psi^u_{r\beta} - \psi^i_{r\beta} \end{cases} \qquad (4)$$

The estimated rotor resistance can be calculated in the adaptation mechanism:

$$r_r^e = \int A_3 dt + A_4 \tag{5}$$

where

$$\begin{cases} A_3 = K_3 \left[\left(\dfrac{-\psi_{r\alpha}^i + x_s i_{\alpha s}}{x_r} \right) \varepsilon_\alpha + \left(\dfrac{-\psi_{r\beta}^i + x_s i_{\beta s}}{x_r} \right) \varepsilon_\beta \right] \\[4mm] A_4 = K_4 \left[\left(\dfrac{-\psi_{r\alpha}^i + x_s i_{\alpha s}}{x_r} \right) \varepsilon_\alpha + \left(\dfrac{-\psi_{r\beta}^i + x_s i_{\beta s}}{x_r} \right) \varepsilon_\beta \right] \end{cases} \tag{6}$$

Parameters K_3 and K_4 are constant positive coefficients. The rotor resistance estimator works if the load torque m_L is not equal to zero.

4. INFLUENCE OF THE ROTOR FAULT
ON THE PROPERTIES OF THE SENSORLESS DRIVE

In this part of the paper, the analysis of the rotor faults on the properties of the sensorless induction motor drive is presented. In the simulation tests, a mathematical model of an induction motor with broken rotor bars was used, which has been presented in detail elsewhere [11]. In this model, the rotor bar fault provokes an increase of the rotor resistance that oscillates because it also depends on the actual rotor angle position. The rotor fault was modeled as a full broken rotor bar. The squirrel cage of the tested induction motor has 22 bars. In the simulation tests, the maximum number of broken bars was 8, and only the neighboring rotor bars were broken.

4.1. SENSORLESS DRIVE SYSTEM
WITHOUT AN ADDITIONAL ROTOR RESISTANCE ESTIMATOR

First, the sensorless drive system was tested without an additional rotor resistance estimator. In Figure 4, the transients of the state variables for broken rotor bars are presented. During the simulation tests, the induction motor was under the constant load torque $m_L = m_N$. The rotor faults were simulated starting from 1 broken bar at $t = 1$ s, till 8 broken bars at $t = 8$. The simulation tests were conducted for three reference rotor speeds.

In Figure 4, the transients of the reference, estimated and measured rotor speeds for broken rotors bars are presented (for $\omega_m = 1 - 0.1\omega_{mN}$). The difference between the measured and estimated rotor speed increases upon the number of broken rotor bars.

When the rotor bars are broken, the rotor resistance differs from the nominal value. Because the MRAS^{CC} estimator has no additional rotor resistance estimator, the rotor speed is calculated with some steady state error. Similar results were obtained for the other reference rotor speed. For low reference rotor speed ($\omega_m = 0.1\omega_{mN}$), the steady error can be so serious that it can cause unstable operation of the sensorless drive system.
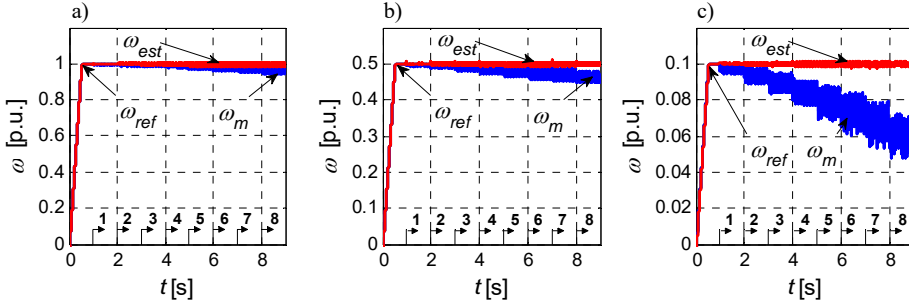

Fig. 4. Transients of reference, measured and estimated rotor speed of DFOC structure for rotor fault in the drive with MRAS^{CC} speed estimator without additional rotor resistance estimator for: a) $\omega_m = \omega_{mN}$, b) $\omega_m = 0.5\omega_{mN}$, c) $\omega_m = 0.1\omega_{mN}$, $m_L = m_N$

Each of the presented signals of the sensorless drive system oscillates with characteristic rotor fault harmonic frequency f_u depending on the actual load torque and fault level, but it does not depend on the actual rotor speed [1, 10]. In Figures 5a, b, the FFT spectrum of the stator current i_{sy} component for 2 and 8 broken rotor bars are presented. The relationship between the f_u frequency and the load torque for 2, 4 and 8 broken rotor bars are presented in Fig. 5c. The frequency f_u increases upon the increasing fault level and torque load. For a healthy rotor, this harmonic does not appear in the FFT spectrum of the stator current i_{sy} component. This finding can be used for the system drive diagnostics [1, 10].
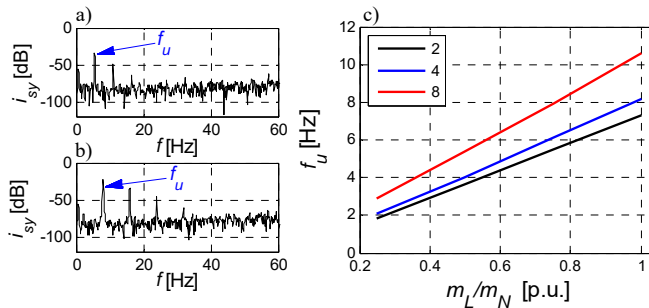

Fig. 5. FFT spectrum of the stator current component i_{sy} for 2 (a) and 8 (b) broken rotor bars for $m_L = m_N$ and the relationship between the frequency of characteristic rotor fault harmonic component and the load torque for 2, 4 and 8 broken rotor bars (c)

4.2. SENSORLESS DRIVE SYSTEM WITH AN ADDITIONAL ROTOR RESISTANCE ESTIMATOR

Another tested system was a sensorless drive with an additional rotor resistance estimator. The block diagram of the rotor speed estimator with additional rotor resistance estimator is presented in Fig. 6. The estimated rotor resistance is additional input for the adjustable model [1]. The estimated rotor resistance was used in the control system at $t = 0.5$ s after the transient state. Results are presented in Figs. 7–9.
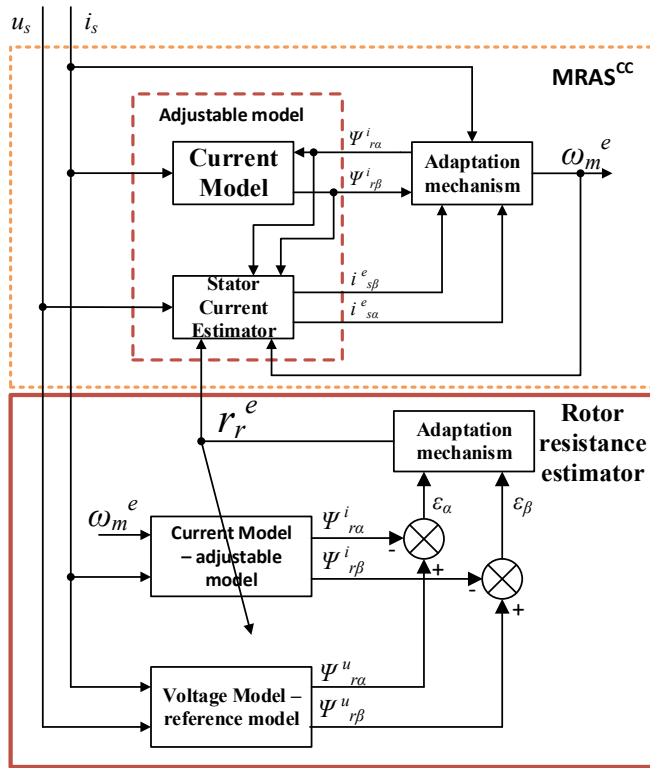
Fig. 6. Scheme of a MRAS^{CC} rotor speed estimator with an additional resistance estimator [1]

In Figures 7a, b, the transients of the reference, estimated and measured rotor speeds for broken rotors bars are presented (for $\omega_m = \omega_{mN}$). The difference between the measured and estimated rotor speeds is approximately equal to zero, independently of the number of broken bars. It is also visible that the estimated and measured rotor speed oscillations increase upon increasing the fault level. In Figure 7c, the transients of real, estimated and nominal values of the rotor resistance are presented. The estimated rotor resistance increases upon the increasing number of broken rotor bars. The estimated rotor resistance can be used as an additional parameter for system drive diagnostics to detect rotor faults [1, 6, 12].
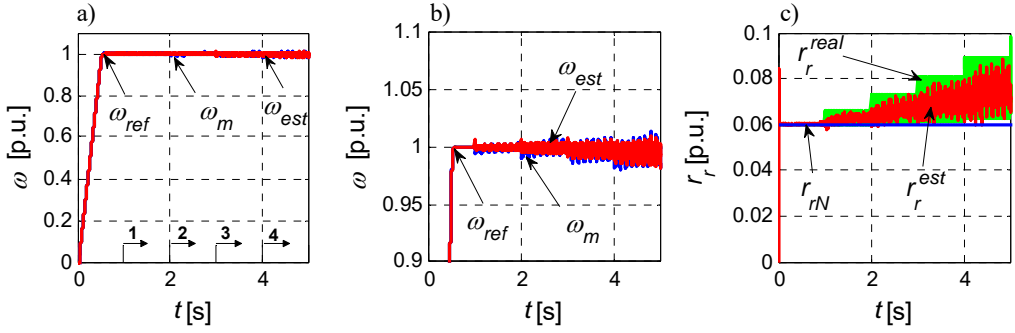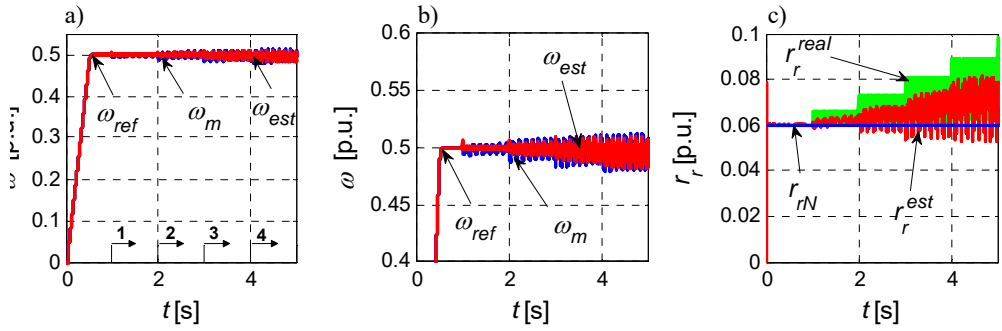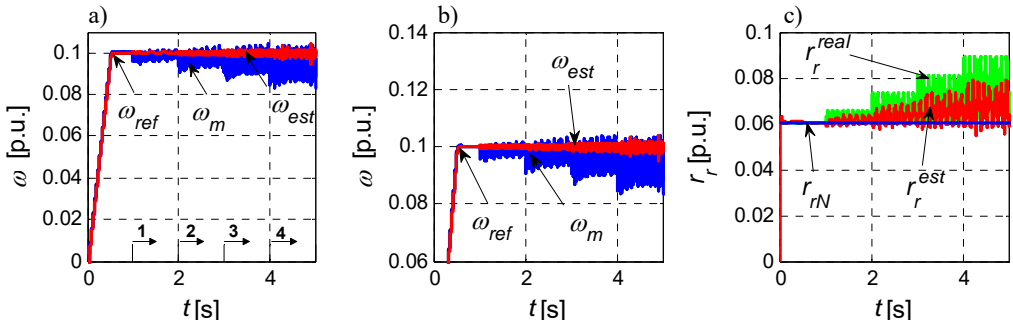
Fig. 7. Transients of reference, measured and estimated rotor speeds (a, b),
real, estimated and nominal rotor resistances (c) for rotor fault in the drive with MRAS^{CC}
speed estimator with an additional rotor resistance estimator for $\omega_m = \omega_{mN}$, $m_L = m_N$

Fig. 8. Transients of reference, measured and estimated rotor speeds (a, b),
real, estimated and nominal rotor resistances (c) for rotor fault in the drive
with MRAS^{CC} speed estimatorwith an additional rotor resistance estimator
for $\omega_m = 0{,}5\omega_{mN}$, $m_L = m_N$

Fig. 9. Transients of reference, measured and estimated rotor speeds (a, b),
real, estimated and nominal rotor resistances (c) for rotor fault in the drive
with MRAS^{CC} speed estimator with an additional rotor resistance estimator
for $\omega_m = 0.1\omega_{mN}$, $m_L = m_N$

Similar results obtained for the other reference rotor speed (Figs. 8 and 9). For a low reference rotor speed ($\omega_m = 0.1\omega_{mN}$), the steady error value is not approximately equal to zero but the sensorless drive system works stably.

5. CONCLUSIONS

The simulation results show that the quality of rotor speed estimation in the sensorless DFOC drive system with a MRAS^{CC} estimator is sensitive to rotor faults. When the rotor bars are broken, the rotor resistance is different from the nominal value. Because the MRAS^{CC} has no additional rotor resistance estimator, the rotor speed is calculated with some steady state error.

In the sensorless DFOC drive system with a MRAS^{CC} estimator and an additional resistance estimator, it is possible to compensate a steady state error but only in limited range of the rotor fault. However, it is important that the estimated rotor resistance can be used as an additional parameter for system drive diagnostics to detect a rotor fault.

Because the speed is calculated correctly, it is possible to detect other faults in the FTC system by the diagnostic systems based on the difference between measured and estimated speed (speed sensor faults).

APPENDIX

Table 1. Parameters of the induction motor

$P_N = 1.1$ kW	$n_N = 1400$ rpm	$R_s = 5.9\ \Omega$	$X_r = 131.1\ \Omega$	$r_s = 0.0778$ p.u.	$x_r = 1.7281$ p.u.
$U_N = 220/380$ V	$f_N = 50$ Hz	$R_r = 4.559\ \Omega$	$X_m = 123.3\ \Omega$	$r_r = 0.0601$ p.u.	$x_m = 1.6253$ p.u.
$I_N = 5.0/2.9$ A	$p_b = 2$	$X_s = 131.1\ \Omega$		$x_s = 1.7281$ p.u.	

REFERENCES

[1] DYBKOWSKI M., *Estimation of speed in a vector controlled induction motor drive – selected problems*, Scientific Papers of the Institute of Electrical Machines, Drives and Measurements of Wrocław University of Technology, No. 67, ser. Monographs, No. 20, Wrocław, Poland, 2013 (in Polish).

[2] FAN S., ZOU J., *Sensor fault detection and fault tolerant control of induction motor drives for electric vehicles*, Proc. 7th International Power Electronics and Motion Control Conference (IPEMC), Harbin, China, June 2012, 1306–1309.

[3] JIANG J., XIANG Y., *Fault-tolerant control systems. A comparative study between active and passive approaches*, Ann. Rev. Control, 2012, 36 (1), 60–72.

[4] JIANG L., *Sensor fault detection and isolation using system dynamics identification techniques*, PhD thesis, The University of Michigan, 2011.

[5] KLIMKOWSKI K., DYBKOWSKI M., *Fault tolerant control structure for induction motor drive system*, Automatika – J. Control, Measure., Electr., Comp. Comm., 2016, 57 (3), 638–647.

[6] KOWALSKI C.T., *Diagnostics of the induction motor drives using artificial intelligence methods*, Oficyna Wydawnicza Politechniki Wrocławskiej, Wrocław, Poland, 2013 (in Polish).

[7] LEE K.S., RYU J.S., *Instrument fault detection and compensation scheme for direct torque controlled induction motor drives*, IEEE Proc. Control Theory Appl., 2003, 150 (4), 376–382.

[8] ORŁOWSKA-KOWALSKA T., *Sensorless induction motor drives*, Oficyna Wydawnicza Politechniki Wrocławskiej, Wroclaw, Poland, 2003 (in Polish).

[9] ORŁOWSKA-KOWALSKA T., DYBKOWSKI M., *Stator current-based MRAS estimator for a wide range speed-sensorless induction motor drive*, IEEE Trans. Ind. Electr., 2009, 57 (4), 1296–1308.

[10] ORŁOWSKA-KOWALSKA T., DYBKOWSKI M., KOWALSKI C.T., *Rotor fault analysis in the sensorless field oriented controlled induction motor drive*, Automatika – J. Control, Measure., Electr., Comp. Comm., 2010, 57 (2), 149–156.

[11] PAWLAK M., ORŁOWSKA-KOWALSKA T., *Application of the simplified two axial model for rotor faults modeling of the induction motor*, Electr. Rev., 2006, 82 (10), 48–53.

[12] WIERZBICKI R., *Diagnostics of the induction motor using state variable and parameter estimators*, PhD thesis, Wrocław University of Technology, Wrocław 2011 (in Polish).

[13] ZORGANI Y.A., KOUBAA Y., BOUSSAK M., *Simultaneous estimation of speed and rotor resistance in sensorless ISFOC induction motor drive based on MRAS scheme*, ICEM, Rome 2010.